PHYSICAL REVIEW D

PARTICLES AND FIELDS

THIRD SERIES, VOLUME 39, NUMBER 2 15 JANUARY 1989

Cosmic-string-loop fragmentation

Robert J. Scherrer

Harvard-Smithsonian Center for Astrophysics and Department of Physics, Harvard University, Cambridge, Massachusetts 02138 and Theoretical Astronomy Unit, Queen Mary College, London, England

William H. Press

Harvard-Smithsonian Center for Astrophysics and Department of Physics, Harvard University, Cambridge, Massachusetts 02138

(Received 1 July 1988)

We present the results of a numerical simulation of the fragmentation of single cosmic-string loops in flat spacetime. The analytic solution for the motion of the fragmenting loop is derived, and this solution is followed forward to determine the trajectories of the daughter loops. We find that loop fragmentation is not stochastic; the loop fragmentation probability decreases with fragmentation generation, and a universal loop fragmentation probability is not well defined. All of the loops sampled eventually reached nonintersecting trajectories. We see no evidence for fragmentation down to arbitrarily tiny loops. The final loop size distribution is approximately a lognormal distribution. The mean final loop velocity is $v \sim 0.6c$.

I. INTRODUCTION

Cosmic strings are topological defects which may form during a phase transition in the early Universe; they are of interest as possible seeds for the formation of galaxies and large-scale structure (see Ref. 1 for a recent review). However, an understanding of the astrophysical effects of cosmic strings requires a knowledge of the way in which strings form during the phase transition and evolve to the epoch of galaxy formation. While the initial configuration of cosmic strings is relatively well understood,[2-5] considerably more uncertainty remains regarding cosmic-string evolution. The nonlinear partial differential equations governing string motion in an expanding background have been studied both numerically[6,7] and analytically.[8,9] The analytic work, based on considerations of energy transfer in the string network between long strings and closed loops, provides insight into the gross features of string evolution, but it cannot be applied to detailed questions regarding the spatial distribution of the strings. The full numerical integrations of the string equations of motion by Albrecht and Turok[6] and Bennett and Bouchet[7] provide the most detailed information regarding string evolution, but they are limited in their ability to resolve the behavior of the smallest loops in the simulation.

In this paper we deal with a much simpler problem: the evolution of a single loop well inside the horizon. In this case, the equations of motion can be solved analytically, and the motion of the daughter loops which form from the fragmentation of the original loop can be calculated analytically from the original string trajectory. This approach is complementary to the Albrecht-Turok and Bennett-Bouchet simulations. Those simulations indicate that loops typically form with radii smaller than the horizon. Our simulation allows us to evolve such loops forward with high accuracy to determine their ultimate fate.

The main questions of interest are whether typical loops cease fragmenting at some point, or continue to chop themselves up into smaller and smaller pieces, and whether or not there exists a "universal" fragmentation probability for the loop trajectories. Previous discussions of the behavior of cosmic strings in flat spacetime are given in Refs. 10–15.

In the next section we derive the solution for the equations of motion governing a fragmenting loop, and we indicate how the trajectories of the daughter loops are related to the original loop trajectory. Our numerical simulation is described in Sec. III, and our results and conclusions are presented in Sec. IV.

II. EQUATIONS OF MOTION FOR A FRAGMENTING LOOP

Consider the trajectory of an isolated cosmic-string loop well inside the horizon.[16] The motion of the loop can be parametrized in terms of two independent variables: σ, the invariant length along the string, which is proportional to the energy of the string measured along the string from a fixed point, and t, the time. The trajectory of the string is given by $\mathbf{x}(\sigma,t)$, the position in three-dimensional space of the point σ on the string at the time t. In flat spacetime, the equation of motion for the string takes the simple form

$$\ddot{\mathbf{x}}=\mathbf{x}'' , \tag{1}$$

with the gauge conditions

$$\dot{\mathbf{x}}\cdot\mathbf{x}'=0 , \tag{2a}$$

$$\dot{\mathbf{x}}^2+\mathbf{x}'^2=1 , \tag{2b}$$

where $\dot{\mathbf{x}}=\partial\mathbf{x}/\partial t$ and $\mathbf{x}'=\partial\mathbf{x}/\partial\sigma$. The general solution to Eqs. (1) and (2) is

$$\mathbf{x}=\tfrac{1}{2}[\mathbf{a}(\sigma+t)+\mathbf{b}(\sigma-t)] , \tag{3}$$

where $\mathbf{a}$ and $\mathbf{b}$ are arbitrary functions satisfying $\mathbf{a}'^2=\mathbf{b}'^2=1$ and $\mathbf{a}(\sigma+L)=\mathbf{a}(\sigma)$, $\mathbf{b}(\sigma+L)=\mathbf{b}(\sigma)$; L is the total invariant length of the string loop. Thus $\mathbf{a}$ and $\mathbf{b}$ are simply arbitrary closed curves of equal length parametrized by their length.

The condition for the string to intersect itself is

$$\mathbf{x}(\sigma_1,t)=\mathbf{x}(\sigma_2,t) . \tag{4}$$

In terms of the $\mathbf{a}$ and $\mathbf{b}$ functions, this becomes

$$\mathbf{a}(\sigma_1+t)+\mathbf{b}(\sigma_1-t)=\mathbf{a}(\sigma_2+t)+\mathbf{b}(\sigma_2-t) . \tag{5}$$

It is convenient to work in terms of the variables σ_A, σ_B, and Δ defined by $\sigma_A=\sigma_1+t$, $\sigma_B=\sigma_1-t$, and $\Delta=\sigma_2-\sigma_1$. Then Eq. (5) can be rewritten as

$$\mathbf{a}(\sigma_A+\Delta)-\mathbf{a}(\sigma_A)=\mathbf{b}(\sigma_B)-\mathbf{b}(\sigma_B+\Delta) . \tag{6}$$

Because the $\mathbf{a}$ and $\mathbf{b}$ curves have $\mathbf{a}'^2=\mathbf{b}'^2=1$, Eq. (6) has a simple geometrical interpretation: self-intersection of the loop occurs if there exist points A_1,A_2 on curve $\mathbf{a}$ and B_1,B_2 on curve $\mathbf{b}$ for which the arc lengths from A_1 to A_2 and B_1 to B_2 are equal, and the chords from A_1 to A_2 and B_1 to B_2 have the same length and direction (see Fig. 1).

Suppose that self-intersection does occur. It is thought that the probability for two intersecting string segments to break and exchange partners upon reconnection is quite close to unity,[17] and we shall assume in this paper that such an exchange of partners always occurs, so that each self-intersection of a single loop produces two "daughter" loops. Each daughter loop also obeys Eqs. (1) and (2) and can be characterized in terms of a solution of the form given by Eq. (3). Suppose that the original loop is defined by the curves $\mathbf{a}$ and $\mathbf{b}$ and fragments at a time t at points σ_1 and σ_2. It will be convenient to work in terms of σ_A, σ_B, and Δ defined above. After fragmentation occurs, consider the daughter loop corresponding to the points $\sigma_1\le\sigma\le\sigma_2$ on the parent loop, or equivalently, the points $\sigma_A\le\sigma\le\sigma_A+\Delta$ on curve $\mathbf{a}$ and $\sigma_B\le\sigma\le\sigma_B+\Delta$ on curve $\mathbf{b}$. This daughter loop is characterized by the new curves $\mathbf{a}_n$ and $\mathbf{b}_n$. The position and velocity of this daughter loop immediately after fragmentation are identical to the position and velocity of the parent loop immediately prior to fragmentation, so we must have

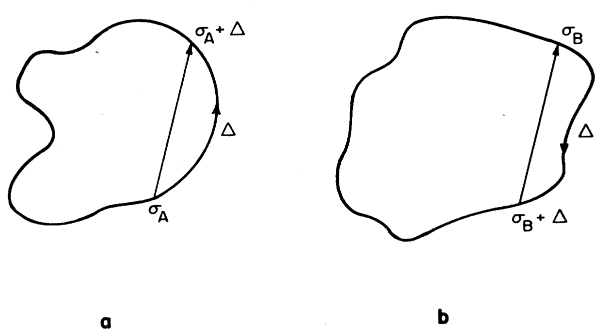

FIG. 1. The cosmic loop defined by the curves $\mathbf{a}$ and $\mathbf{b}$ intersects itself because the arcs $\sigma_A,\sigma_A+\Delta$ and $\sigma_B,\sigma_B+\Delta$ have equal length Δ, and the chords from σ_A to $\sigma_A+\Delta$ and σ_B to $\sigma_B+\Delta$ have equal length and direction.

$$\mathbf{a}_n(\sigma)=\mathbf{a}(\sigma) \tag{7a}$$

for $\sigma_A\le\sigma\le\sigma_A+\Delta$ and

$$\mathbf{b}_n(\sigma)=\mathbf{b}(\sigma) \tag{7b}$$

for $\sigma_B\le\sigma\le\sigma_B+\Delta$. However, the daughter loop has a new invariant length Δ, and so the position and velocity of the loop must be periodic with period Δ:

$$\mathbf{a}_n(\sigma+\Delta)+\mathbf{b}_n(\sigma+\Delta)=\mathbf{a}_n(\sigma)+\mathbf{b}_n(\sigma) , \tag{8a}$$

$$\mathbf{a}'_n(\sigma+\Delta)-\mathbf{b}'_n(\sigma+\Delta)=\mathbf{a}'_n(\sigma)-\mathbf{b}'_n(\sigma) , \tag{8b}$$

for all σ. The solution to Eq. (8) is

$$\mathbf{a}_n(\sigma+\Delta)=\mathbf{a}_n(\sigma)+\mathbf{d} , \tag{9a}$$

$$\mathbf{b}_n(\sigma+\Delta)=\mathbf{b}_n(\sigma)-\mathbf{d} , \tag{9b}$$

where $\mathbf{d}$ is the constant vector defined by the intersection points on the original loop:

$$\mathbf{d}=\mathbf{a}(\sigma_A+\Delta)-\mathbf{a}(\sigma_A)=\mathbf{b}(\sigma_B)-\mathbf{b}(\sigma_B+\Delta) .$$

Thus, while the daughter loop can be described by Eq. (3), the new $\mathbf{a}$ and $\mathbf{b}$ curves are no longer closed curves. Again, Eqs. (7) and (9) have a simple geometric interpretation (see Fig. 2). When fragmentation occurs, the $\mathbf{a}$ and $\mathbf{b}$ curves fragment at the points $\sigma_A,\sigma_A+\Delta$ and $\sigma_B,\sigma_B+\Delta$, and the sections of the $\mathbf{a}$ and $\mathbf{b}$ curves which lie between these fragmentation points are simply extended periodically in space to form the new curves $\mathbf{a}_n$ and $\mathbf{b}_n$. The velocity of the new daughter loop appears naturally in this derivation. From Fig. 2, it is clear that the center of mass of the daughter loop is displaced by a distance $\mathbf{d}$ during a single loop period Δ, so the velocity of the center of mass of the daughter loop relative to the parent loop is simply $\mathbf{d}/\Delta$ (in units where $c=1$). Velocities near 1 correspond to arcs which are almost straight lines, and it is clear geometrically that $\mathbf{d}/\Delta$ is always less than 1.

This derivation indicates a relation between fragmentations of the daughter loops and self-intersections of the parent loop. Suppose that the intercommutation proba-

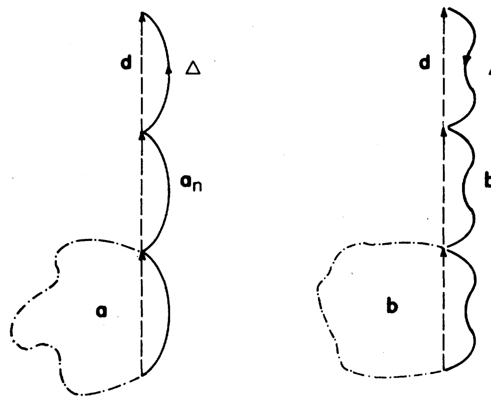

FIG. 2. After self-intersection, the new curves $\mathbf{a}_n$ and $\mathbf{b}_n$ are derived by extending the corresponding sections of the old **a** and **b** curves periodically in space. The velocity of the daughter loop is $\mathbf{d}/\Delta$.

bility were 0, so that the parent loop could self-intersect without fragmenting. Then each self-intersection of the parent loop would correspond to a geometrical configuration such as that shown in Fig. 1. However, since a given daughter loop is composed of segments from the **a** and **b** curves of the parent loop, self-intersection of the daughter loop corresponds to a self-intersection in the trajectory of the initial parent loop. See Fig. 3; the points A_1, A_2, B_1, B_2 correspond to a self-intersection of the indicated daughter loop. On the other hand, they would also correspond to a fragmentation of the parent loop if this parent loop had not already fragmented. In fact, it is possible for fragmentation to eliminate potential intersection points. See Fig. 4; the points A_1, A_2, B_1, B_2 and A_3, A_4, B_3, B_4 both satisfy condition (6) and therefore both represent self-intersections of the parent loop trajectory. However, when the daughter loop corresponding to A_1, A_2, B_1, B_2 fragments off of the parent loop, the points A_3, B_3 and A_4, B_4 end up on different loops, so they do not correspond to self-intersection of any daughter loops.

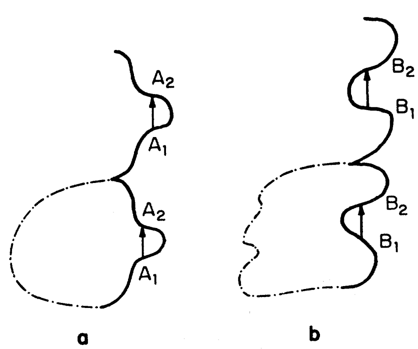

FIG. 3. The points A_1, A_2, B_1, B_2 correspond to a self-intersection of the daughter loop which was also a self-intersection of the parent loop.

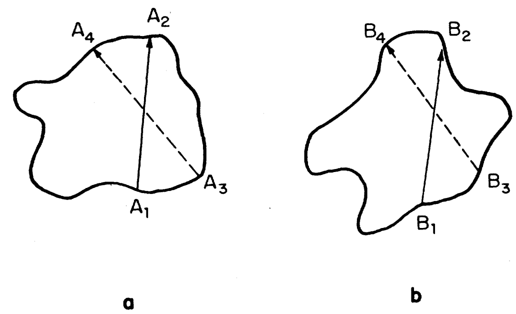

FIG. 4. The elimination of an intersection point through fragmentation: the fragmentation at A_1, A_2, B_1, B_2 eliminates the potential self-intersection at A_3, A_4, B_3, B_4.

If this were the only process operating, then the number of self-intersections of the parent loop trajectory would represent an upper bound on the number of daughter loops produced by fragmentation. However, it is also possible for fragmentation to produce new self-intersections in the loop trajectories. Consider the daughter loop trajectory shown in Fig. 5. The points A_1, A_2, B_1, B_2 satisfy Eq. (6) and therefore represent a self-intersection of the daughter loop. However, this self-intersection was not present in the initial parent loop trajectory. The reason is that A_1 and A_2 straddle the intersection point, while B_1 and B_2 do not. Thus A_1 and A_2 have been displaced relative to each other by the production of this daughter loop, producing a new intersection. [If both A_1, A_2 and B_1, B_2 straddled the intersection point, one could simply translate A_2 and B_2 by the vector **d** (Fig. 2) and arrive at an intersection point which was also present in the parent loop trajectory.]

It is clear that the creation and destruction of intersection points are crucial to the eventual fate of the fragmenting loop. It is often assumed[9,11] that the behavior of a fragmenting loop is stochastic; i.e., the fragmentation probability for all the daughter loops produced in a cas-

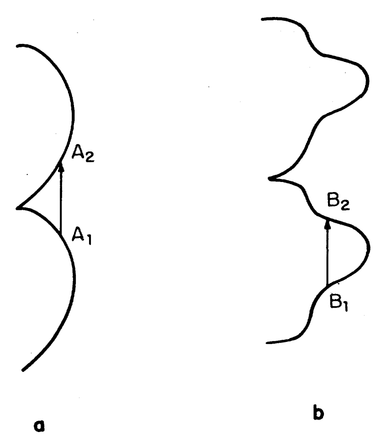

FIG. 5. The creation of a new intersection point through fragmentation: the self-intersection of the daughter loop at A_1, A_2, B_1, B_2 was not present in the initial parent loop.

cade of fragmentations can be characterized by a single number q. Although our formalism clearly indicates the deterministic nature of the trajectories of the fragmenting loops, the fragmentation could appear stochastic if the creation and destruction of intersection points with each fragmentation were sufficiently high as to represent a new "throw of the dice." On the other hand, if the creation of new intersections occurs at a low enough rate, the fragmentation probability will decrease with each generation and the fragmentation process will eventually come to a halt. These questions will be addressed in Sec. IV.

III. THE NUMERICAL SIMULATION

We work only with the analytic equations of motion given by Eq. (3). Then the procedure outlined in the previous section allows us to calculate the trajectories of the fragmenting loops as accurately as desired. The disadvantage of such an approach is that it requires specific assumptions regarding the type of loop trajectories to be sampled. For this project, we have chosen to sample two widely different sets of loop trajectories. We will draw general conclusions only about the results which are common to both sets of trajectories. We work in terms of the **a** and **b** functions, which we express in the form

$$a_x(s)=\sum_{m=1}^{M} a_{xm}\cos(ms+\phi_{xm}) , \tag{10a}$$

$$b_x(s)=\sum_{m=1}^{M} b_{xm}\cos(ms+\phi_{xm}) , \tag{10b}$$

and similarly for the y and z components. The ϕ_m's are random numbers chosen uniformly between 0 and 2π. The two cases sampled here are (A) a set of trajectories with large high-frequency modes: we take $M=10$ and the a_m's and b_m's are random numbers chosen uniformly between 0 and 1 and (B) a set of trajectories with little high-frequency amplitude: $M=10$ and the a_m's and b_m's are random numbers chosen uniformly between 0 and $1/m^2$. In Eq. (10), s does not give the length along the curve, so we calculate $\sigma(s)$ numerically. The **a** and **b** curves are then normalized to have the same length. A loop of each type is shown in Fig. 6.

To evolve the loop, we set down N points along the **a** and **b** curves at equal intervals (for this project, we take $N=128$). The evolution of these N points is followed using the analytic solution [Eq. (3)]. We check for self-intersection by examining when the straight segments connecting the N points cross. To check for crossing of two segments, we calculate the volume of the tetrahedron defined by the four end points of the segments. When this volume goes through zero, the segments are coplanar and can then be checked to determine if they actually intersect. This is the same procedure as that used by Bennett and Bouchet.[7] This procedure essentially amounts to approximating the smooth **a** and **b** curves by closed curves consisting of N straight chords of equal length. Because this approximation does not follow the path of the **a** and **b** curves exactly, particularly near kinks, it can lead to small errors in the determination of the location of the exact points of intersection on the **a** and **b** curves,

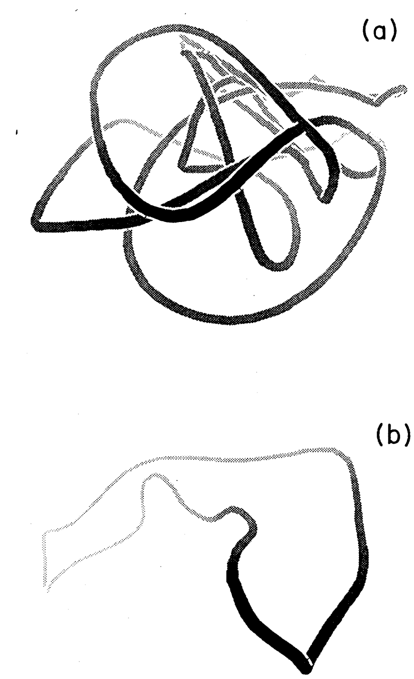

FIG. 6. Typical initial loop configurations for (a) case A and (b) case B. Thicker and darker sections of the loop are closer to the viewer.

or even to spurious intersections. In practice, it was found that the future trajectory of the curve was extraordinarily sensitive to small perturbations in the location of the intersection points. Consequently, after a crossing is discovered, we solve Eq. (6) using the Newton-Raphson method to calculate exactly where to fragment the **a** and **b** curves. After the fragmentation points are determined, the new **a** and **b** curves for the daughter loops are determined using the procedure outlined in the preceding section. We then set down N points on each of the new daughter loops and evolve the new trajectories as described above.

Because all daughter loop trajectories are expressed in terms of the original analytic expressions for the **a** and **b** curves, the only loss of accuracy which arises due to the fragmentation process comes from the error in calculating the fragmentation points on the **a** and **b** curves. Since all loops in the simulation are divided into the same number of segments, regardless of their size, the evolution of the smallest loops should not be any less accurate than that of the initial parent loop. On the other hand, this procedure does introduce a minimum cutoff on the ratio of daughter loop size to the parent loop size for a single fragmentation: a parent loop cannot produce a daughter loop smaller than $\sim 1/N$ of the parent loop size in a single fragmentation. However, multiple fragmentation can produce much smaller loops: we observe daughter loops as small as 0.0003 of the parent loop size.

Because we are interested in the behavior of isolated loops, we have ignored any interaction between the fragmenting loops and other cosmic strings. In addition, it is impractical to resolve loop fragmentation to the accuracy we have used here and also to check for reconnections between daughter loops produced from the same parent loop. We have chosen to sacrifice the latter in favor of the former. However, reconnection of the daughter loops could have a significant effect on the final loop trajectories, so we have estimated this effect using a much cruder form of the simulation ($N=16$ and 32) and checking for reconnection among the daughter loops. We do not actually reconnect the loops, but simply calculate the fraction of all of the daughter loops (stable and unstable) which intersect any other daughter loops in the course of the simulation. Sampling 10% of the trajectories discussed in the next section, we find that reconnection is very rare for case B; fewer than $\frac{1}{10}$ of the daughter loops intersected each other in the course of the simulation. Loop velocities tend to separate the daughter loops after fragmentation. As expected, reconnection is much more common in case A; roughly $\frac{2}{3}$ of all of the daughter loops intersected each other. However, almost all of these intersections took place in the initial stages of the simulation. This suggests that the string configuration eventually becomes sufficiently untangled that there is a regime over which our results are applicable. These conclusions must be considered less reliable than the rest of our results, due to the crudeness of this form of the simulation.

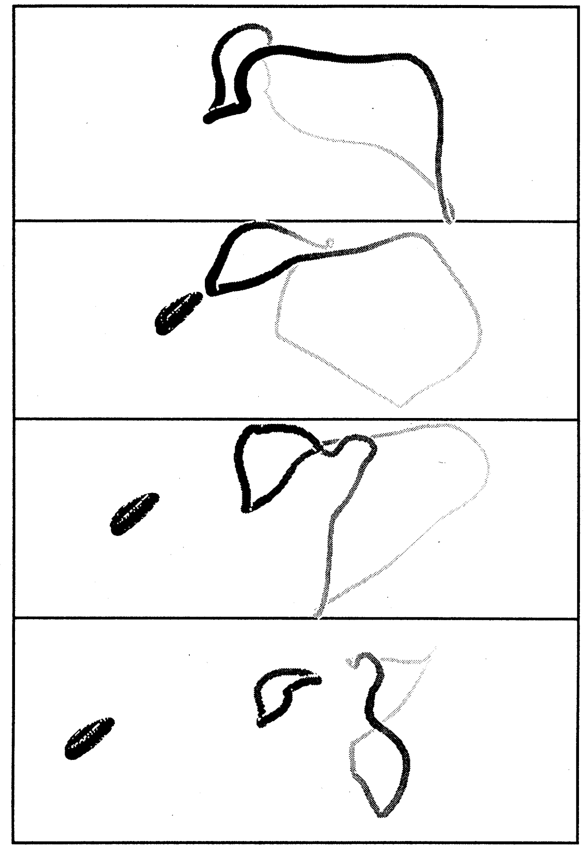

FIG. 7. Part of the evolution of a type-B loop, at time intervals of $\frac{6}{64}$ of the parent loop period. Thicker and darker sections of the loop are closer to the viewer.

IV. RESULTS AND CONCLUSIONS

Using the procedure outlined above, we have fragmented 20 parent loops of type A and 80 parent loops of type B. Part of the evolution of one of the type-B loops is shown in Fig. 7. All of the initial type-A parent loops were self-intersecting, while 5 of the 80 initial type-B parent loops were stable. The total number of final stable daughter loops was 561 (case A) and 611 (case B). The mean number and standard deviation of stable daughter loops produced from each parent loop was 28 ± 6 for case A and 8 ± 4 for case B. Clearly, the mean number of stable daughters produced per parent is strongly dependent on the initial loop configuration; as expected, a loop with higher-frequency modes will produce more daughter loops.

Whenever a fragmentation occurs, we can define a fragmentation fraction f given by the ratio of the length of the smaller of the two daughter loops to the length of the parent loop. The fraction f $(0<f\leq 0.5)$ gives a measure of whether loops break roughly in half ($f=0.5$) or whether they tend to break off tiny daughter loops ($f\simeq 0$). The number of fragmentations with a given value of f is shown in Figs. 8(a) and 8(b) for cases A and B, respectively. For both cases investigated, the fragmentation fraction is relatively flat; i.e., a loop is equally likely to fragment anywhere along its length. There is no tendency for the loop to break approximately in half, nor does the loop tend to break off tiny daughter loops. There is an artificial lower cutoff on f produced by our procedure for finding fragmentations ($f \gtrsim 1/N$); this produces a sharp decrease in the smallest bin in both 8(a) and 8(b). However, the number of fragmentations as a function of f is not increasing sharply just above this cutoff, and doubling the number of segments to $N=256$ did not produce a large increase in such small fragmentations. We therefore conclude that we are not missing a large number of fragmentations just below our cutoff. On the other hand, we cannot rule out the production of tiny loops far below the size resolution of our simulation, but such loop production would be difficult to detect in any numerical simulation.

As noted in Sec. III, one of the most important questions regarding loop fragmentation is whether or not it is stochastic; i.e., can we assign a loop fragmentation probability q which is a constant throughout the fragmentation process? It is clear from the discussion in Sec. III that this is not the most natural assumption. Stochastic loop fragmentation would require the number of fragmentation points on each daughter loop to be roughly equal throughout the fragmentation process. This means that the number of fragmentation points per unit invariant length would have to increase sharply with each fragmentation. If the creation of fragmentation points were equal to the destruction of such points, the number of fragmentation points per comoving length would remain roughly constant, and the fragmentation probability q would decrease with each fragmentation. Stochastic fragmenta-

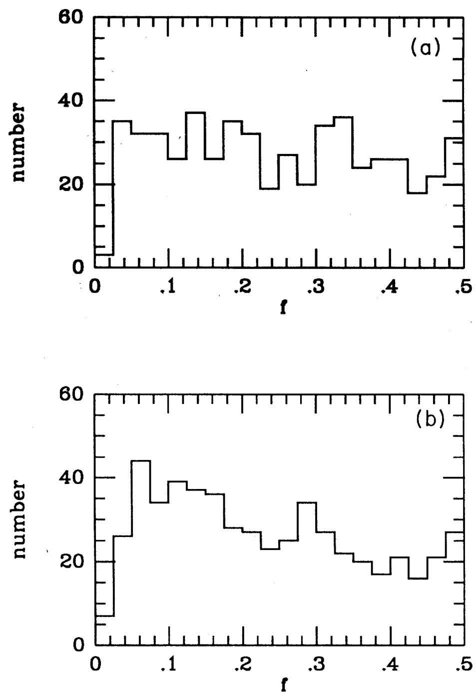

FIG. 8. The number of fragmentations with a given fragmentation fraction f, where f is the ratio of the length of the smaller of the two daughter loops to the length of the immediate parent loop, for (a) case A and (b) case B.

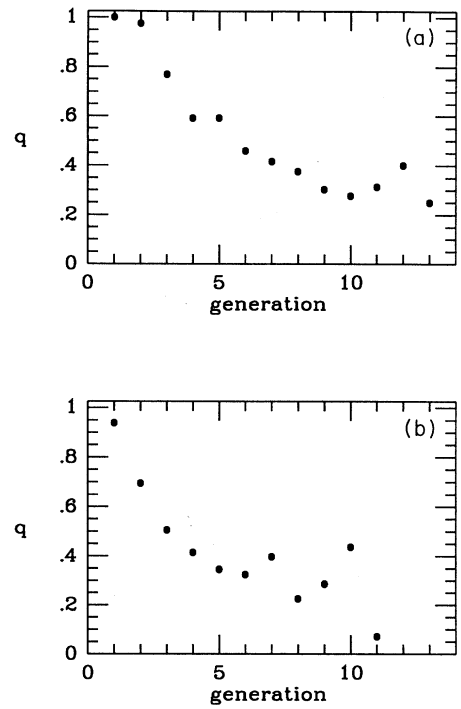

FIG. 9. The fragmentation probability q as a function of loop generation for (a) case A and (b) case B.

tion would require a much larger rate for the creation of fragmentation points than for their destruction.

A graph of the fragmentation probability q as a function of generation is given in Fig. 9 for the two cases sampled. (A loop belongs to the nth generation if it resulted from $n-1$ fragmentations.) For this graph, we have retained generations containing ten or more loops. It is clear that the fragmentation probability decreases with generation for both cases studied. Loop fragmentation is not stochastic, and a universal fragmentation probability for the loops is not well defined.

Further evidence for the nonstochastic nature of the loop fragmentation is given by the size distribution of the stable daughter loops. The invariant length distribution for these loops is given in Figs. 10(a) and 10(b) for cases A and B, respectively. Although the mean loop size is smaller in case A than in case B, the shape of the size distribution is similar in both cases. In neither case do we see fragmentation down to arbitrarily small loops; all of our simulations eventually reached a state containing only stable daughter loops.

Stochastic fragmentation with a flat fragmentation fraction as given in Fig. 8 would produce a power-law distribution of sizes.[18] Let L be the size of the final daughter loop in units in which the initial parent loop has unit invariant length. The distribution of sizes for a single loop after n fragmentations is given by[19]

$$p_n(L)=\frac{[\ln(1/L)]^{n-1}}{(n-1)!}dL \ . \tag{11}$$

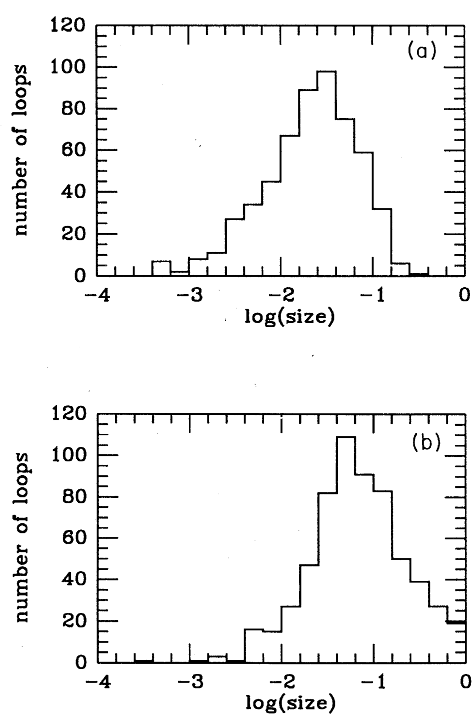

FIG. 10. The number of stable daughter loops as a function of the logarithm of invariant length, in units where the initial parent loop size is 1, for (a) case A and (b) case B.

The mean number of daughter loops produced by exactly n fragmentations is

$$N(n)=(2q)^n(1-q)\ , \tag{12}$$

where q is the stochastic fragmentation probability. Multiplying Eqs. (11) and (12) and summing over n, we obtain the number of loops of a given size L:

$$N(L)=[(1-q)\delta(L-1)+2q(1-q)L^{-2q}]dL\ . \tag{13}$$

Stochastic fragmentation with a flat fragmentation fraction produces a power-law size distribution with exponent between -2 and 0, clearly not what is observed.

However, we can show under quite general assumptions that the observed size distribution must be unimodal. We assume that the fragmentation fraction is always flat throughout the fragmentation process (i.e., it does not depend on generation), but that the fragmentation probability is a decreasing function of generation. Let q_n be the probability for a loop of the nth generation to fragment, and suppose that q_n is a decreasing function of n: $q_1>q_2>q_3>\cdots$. Then the mean number of daughter loops produced by exactly n fragmentations is

$$N(n)=q_1q_2\cdots q_n(1-q_{n+1})2^n\ . \tag{14}$$

Since q_n is a decreasing function of n, $N(n)$ is an increasing function for $q_{n+1}>\frac{1}{2}$ and a decreasing function for $q_{n+1}<\frac{1}{3}$. In addition, if q_n decreases sufficiently gradually for $\frac{1}{2}>q_n>\frac{1}{3}$, then $N(n)$ will have only a single maximum. [The actual condition for this to hold is $q_{n+1}>(3-1/q_n)/2$ whenever $\frac{1}{2}>q_n>q_{n+1}>\frac{1}{3}$.] This condition is satisfied for our loops, as can be seen from Fig. 11, where we give the number of stable daughter loops as a function of their generation. Given a function $N(n)$ with a single maximum, it is easy to show that the size distribution must also have a single maximum. In terms of $z\equiv\ln(1/L)$, we have

$$N(z)=\sum_{n=1}^{\infty}N(n)\frac{z^{n-1}}{(n-1)!}e^{-z}dz\ . \tag{15}$$

Then $N'(z)=\sum_{n=1}^{\infty}[N(n+1)-N(n)]z^{n-1}e^{-z}/(n-1)!$. Descartes's rule of signs says that $\sum[N(n+1)-N(n)]z^{n-1}/(n-1)!$ can have at most as many zeros as $N(n+1)-N(n)$ has changes in sign; if $N(n)$ has a single maximum, then so does $N(z)$.

It is not surprising that the size distributions in Fig. 10 resemble a lognormal distribution. The central limit theorem guarantees that $z^{n-1}e^{-z}/(n-1)!$ will approach a lognormal as $n\rightarrow\infty$. Then if $N(n)$ is sharply peaked about some large n, as it is in Fig. 11, the sum given in Eq. (15) will also approach a lognormal. [A lognormal is a distribution of a random variable x such that $\ln x$ has a normal (i.e., Gaussian) distribution.]

The velocity distribution of the stable daughter loops is given in Fig. 12. The velocity distribution is quite similar for the two cases except at the high-velocity end, where case B produces many more loops with velocities near c. Both cases yield similar mean velocities: $v/c=0.55$

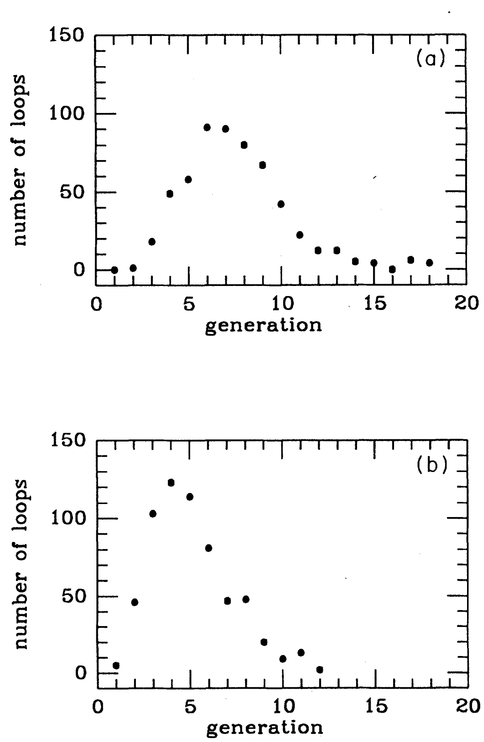

FIG. 11. The number of stable daughter loops belonging to a given generation for (a) case A and (b) case B.

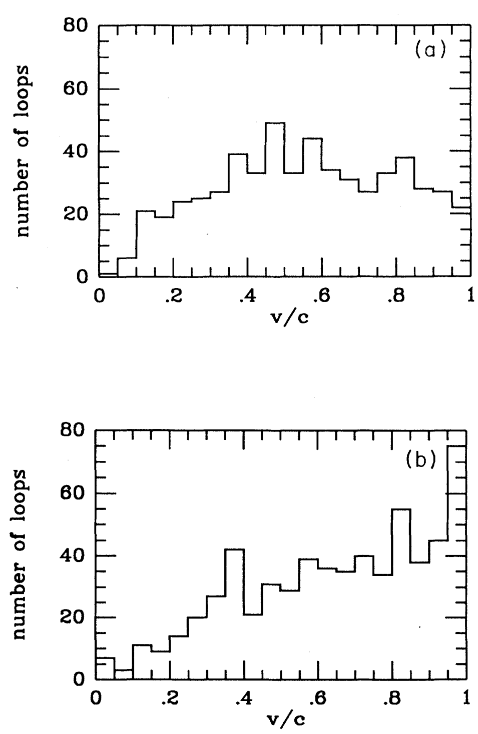

FIG. 12. The number of stable daughter loops with the indicated velocity for (a) case A and (b) case B.

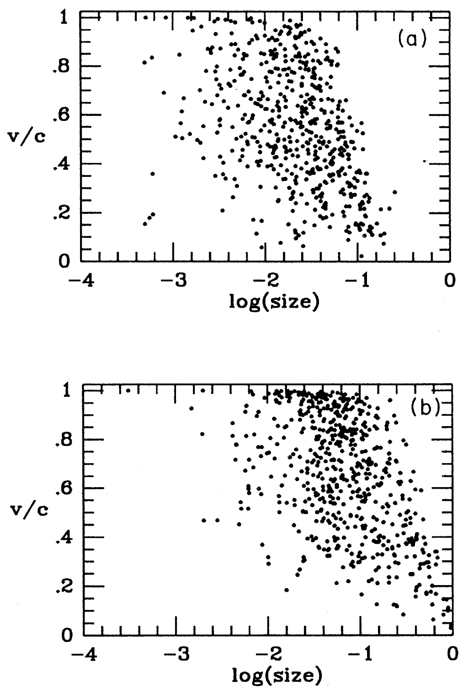

FIG. 13. A scatter plot of velocity vs the logarithm of invariant loop length for the stable daughter loops, in units where the initial parent loop size is 1, for (a) case A and (b) case B.

± 0.24 for case A, and $v/c = 0.64 \pm 0.25$ for case B. These velocities are significantly larger than the mean velocities reported in the Albrecht and Turok simulations,[20] but they are consistent with the more recent results of Bennett and Bouchet.[21] There is a strong correlation between loop size and velocity. In Fig. 13 we give a scatter plot of the velocity versus loop size for all of the stable daughter loops. As expected, the smaller loops tend to have larger velocities. This has a simple explanation in terms of the geometric interpretation of velocity given in Sec. II. When the daughter loop size becomes smaller than the typical radius of curvature for the **a** and **b** curves, the ratio of the chord length to arc length for the daughter loop (Fig. 2) approaches unity. Conversely, large loop velocities are possible only on length scales for which the **a** and **b** curves are nearly straight.

Our results have several implications for models in which strings serve as seeds for the formation of galaxies and large-scale structure. If loop fragmentation continued indefinitely, the string loops would eventually chop themselves into sufficiently small pieces that gravitational radiation would destroy them in less than a Hubble time, eliminating the possibility of matter accreation. Our results indicate that this does not occur, since all of our loops eventually end up in non-self-intersecting configurations. High loop velocities have important implications for the formation of large-scale structure. They tend to destroy the preexisting r^{-2} loop correlations,[20] resulting in a final loop distribution which is essentially random.[22] In addition, such large loop velocities suggest that spherical accretion is a rather poor approximation for cosmic strings; the moving loops will produce more elongated structures.[23] The process of galaxy formation is then more complicated than spherical accretion around static correlated loops.

ACKNOWLEDGMENTS

We thank D. Bennett and F. Bouchet for helpful discussions. This work was supported in part by the National Science Foundation (Grant No. PHY-8604396) at Harvard, and by NATO (R.J.S.) at Queen Mary College.

[1]A. Vilenkin, Phys. Rep. **121**, 263 (1985).
[2]T. Vachaspati and A. Vilenkin, Phys. Rev. D **30**, 2036 (1984).
[3]T. W. B. Kibble, Phys. Lett. **166B**, 311 (1986).
[4]R. J. Scherrer and J. A. Frieman, Phys. Rev. D **33**, 3556 (1986).
[5]E. T. Vishniac, K. A. Olive, and D. Seckel, Nucl. Phys. **B289**, 717 (1987).
[6]A. Albrecht and N. Turok, Phys. Rev. Lett. **54**, 1868 (1985).
[7]D. P. Bennett and F. R. Bouchet, Phys. Rev. Lett. **60**, 257 (1988).
[8]T. W. B. Kibble, Nucl. Phys. **B252**, 227 (1985).
[9]D. P. Bennett, Phys. Rev. D **33**, 872 (1986); **34**, 3592 (1986).
[10]T. W. B. Kibble and N. Turok, Phys. Lett. **116B**, 141 (1982).
[11]A. G. Smith and A. Vilenkin, Phys. Rev. D **36**, 987 (1987); **36**, 990 (1987).
[12]C. Thompson, Phys. Rev. D **37**, 283 (1988).
[13]A. L. Chen, D. A. DiCarlo, and S. A. Hotes, Phys. Rev. D **37**, 863 (1988).
[14]M. Sakellariadou and A. Vilenkin, Phys. Rev. D **37**, 885 (1988).
[15]T. Vachaspati (unpublished).
[16]Some of the results presented in Sec. II have been derived independently by Thompson (Ref. 12).
[17]E. P. S. Shellard, Nucl. Phys. **B283**, 624 (1987).
[18]This calculation was first done by A. van Dalen (unpublished).
[19]W. Feller, *An Introduction to Probability Theory and its Applications* (Wiley, New York, 1966), Vol. II, pp. 24 and 25.
[20]N. Turok, Phys. Rev. Lett. **55**, 1801 (1985).
[21]D. P. Bennett and F. R. Bouchet (private communication).
[22]R. J. Scherrer, A. L. Melott, and E. Bertschinger (unpublished).
[23]E. Bertschinger, Astrophys. J **316**, 489 (1987).